



The laboratory PROGRA2 database to interpret the linear polarization and brightness phase curves of light scattered by solid particles in clouds and layers

Jean-Baptiste Renard, Edith Hadamcik, J.-C. Worms

► To cite this version:

Jean-Baptiste Renard, Edith Hadamcik, J.-C. Worms. The laboratory PROGRA2 database to interpret the linear polarization and brightness phase curves of light scattered by solid particles in clouds and layers. *Journal of Quantitative Spectroscopy and Radiative Transfer*, 2024, 320, pp.108980. <10.1016/j.jqsrt.2024.108980>. <insu-04520704>

HAL Id: insu-04520704

<https://insu.hal.science/insu-04520704v1>

Submitted on 3 Apr 2024

HAL is a multi-disciplinary open access archive for the deposit and dissemination of scientific research documents, whether they are published or not. The documents may come from teaching and research institutions in France or abroad, or from public or private research centers.

L'archive ouverte pluridisciplinaire **HAL**, est destinée au dépôt et à la diffusion de documents scientifiques de niveau recherche, publiés ou non, émanant des établissements d'enseignement et de recherche français ou étrangers, des laboratoires publics ou privés.



Distributed under a Creative Commons CC BY 4.0 - Attribution - International License



The laboratory PROGRA2 database to interpret the linear polarization and brightness phase curves of light scattered by solid particles in clouds and layers

Jean-Baptiste Renard^{a,*}, E. Hadamcik^b, J.-C. Worms^c

^a LPC2E-CNRS, Orléans, France

^b LATMOS-CNRS, Guyancourt, France

^c COSPAR, Paris, France

ARTICLE INFO

Keywords:

Scattering
Polarization
Dust
Solar system

ABSTRACT

Laboratory measurements of the brightness and linear polarization of the light scattered by clouds of particles are necessary to interpret remote sensing measurements of dust in space and in planetary atmospheres. For 30 years, such laboratory measurements were conducted by the PROGRA2 project for particles with different natures, sizes and shapes. The resulting database contains the brightness and linear polarization curves for 170 samples and at 4 wavelengths in the visible and near infra-red domains. The samples cover most of the particles that we expect to find in space and in planetary atmospheres. The particles can be compact, porous or aggregated, with sizes up to hundreds of μm ; the monomers of aggregates can have sizes as small as 10 nm. The measurements were obtained for clouds of randomly oriented particles levitated on the ground conditions by an air draught technique, and under microgravity conditions during parabolic flights. Complementary measurements were obtained for deposited particles in layers to compare the main characteristics of the phase curves using the same sample. After a description of the instruments and of the samples under study, we present the database and the main results already obtained with PROGRA2. The phase curves often differ for deposited and levitating particles. Such phase curves are related to different physical properties of the particles, and can be compared to modelling calculations. In case of aggregated particles, we discuss the influence of the monomers on the phase curves. Finally, the main results obtained for dust analogs of different objects of the solar system are compared to observations.

1. Introduction

Clouds of solid particles can be found almost everywhere in space, and the modifications of the incoming non-polarized light they scatter can be studied in the visible and near infra-red domains (such light sources are the Sun for solar system bodies and the central star for debris or dust disks). A cloud can be defined as an ensemble of particles in suspension (or in levitation); in the present study, the particles are compact or aggregated solid grains and must also be randomly oriented. The measurements of the evolution of the scattered brightness and linear polarization with the scattering angle Θ , or the phase angle α ($\alpha = 180^\circ - \Theta$) by such clouds of particles can provide access to some of their physical properties, such as albedo, mean size, refractive index, porosity, and main composition. These measurements constitute the

scattering or phase curves. They require a specific geometry for the illumination and the sensors, to be able to cover most of the 0° – 180° range, or at least the 10° – 110° range where information was studied for most of the solar system objects [1,2]. In the following, we will use the phase angle instead of the scattering angle since it is commonly used by the planetary science community.

The objects forming clouds of solid particles in the solar system for which phase curves are well-established are comets [3–6], zodiacal cloud [7–9], the Titan atmosphere [10,11], and solid particles in the Earth stratosphere [12]. Recently, phase curves have been obtained for very distant objects, the debris disks around young stars [13–15].

Phase curves are also obtained for asteroids [16–18] or for the surface of objects without a thick atmosphere covered by dust, such as the Moon [19]. In this case, multiple scattering between the particles may

* Corresponding author.

E-mail address: jean-baptiste.renard@cnrs-orleans.fr (J.-B. Renard).

<https://doi.org/10.1016/j.jqsrt.2024.108980>

Received 20 November 2023; Received in revised form 9 March 2024; Accepted 21 March 2024

Available online 24 March 2024

0022-4073/© 2024 The Authors. Published by Elsevier Ltd. This is an open access article under the CC BY license (<http://creativecommons.org/licenses/by/4.0/>).

occur and is dependent on the number density of the particles and on their absorption.

To interpret such remote-sensing measurements, laboratory experiments with representative particles are necessary for well-documented samples and mixtures thereof. These particles should have different physical properties and compositions as close as possible to those encountered in space and in atmospheres. When the shape of the particles is not symmetrical, their individual scattering properties can strongly vary from one particle to another, due to their irregular shape and structure, and to the difference between the refractive indices of their materials. Thus, individual particles must not be considered for laboratory measurements to simulate complex clouds of particles. On the other hand, when considering at least a few dozen particles having random orientations, and when integrating their individual contributions, one can retrieve the mean scattering properties of the cloud, using statistical approaches [20].

Different laboratory experiments have been developed to retrieve the phase curves of levitating clouds of randomly oriented particles in the visible and near infrared domains, and thus to build up databases [21–27]. The measurements must be performed for levitated particles, since their polarization curves can strongly differ from those for deposited particles [25]. Levitation of randomly oriented particles can be achieved by different techniques. The first one is by an airflow that lifts and carries the particles, although such a method could in some particular conditions orient the compact particles larger than several tens of μm for some particular set-ups where the air speed is greater than about 5 m.s^{-1} [28]. Another method consists of lifting the particles by a low-speed air draught inside a vial; such a method works for μm -sized particles and/or high-porosity aggregates [29,30]. Finally, for large compact particles and for aggregates, levitation can be easily obtained under microgravity conditions for particles sealed in a vial under vacuum [31].

We present here the PROGRA2 database that contains linear polarization and brightness phase curves in the visible and near infrared domain, and for a large variety of samples (transparent to very absorbing particles, compact to fluffy particles, and their mixture) to simulate different media in the solar system. The measurements of levitating particles were obtained at ground by the air draught

technique or under microgravity conditions, depending on the size and density of the particles. Complementary measurements were also carried out for deposited particles, to point out the main differences with the scattered properties of levitating particles and compare them with remote observations of some solar system bodies.

2. The PROGRA2 instruments

The project started in 1993 and ended in 2022. Three versions of the instrument were developed: PROGRA2-Vis for measurements in the visible domain, PROGRA2-IR for measurements in the near infrared domain, and PROGRA2-Surf for measurements in the visible domain of deposited particles (PROGRA2 is a French acronym for optical properties of astronomical and atmospheric particles). All these instruments are transportable and can be used for particles of different kinds (even dangerous ones like asbestos, in this case a specific design to prevent them from being released in the ambient air must be used).

PROGRA2-Vis and IR use the same measurement principle (Fig. 1). The light sources were initially randomly polarized lasers and, in a later version of the instruments, a white lamp combined with a depolarizer and spectral filters to select the wavelength. The wavelengths are 540 nm, 640 nm, 950 nm and 1500 nm. An optical fiber carries the light to the vial in which the particles are contained. The particles scatter the light when they are lifted and cross the light beam. A polarizing beam splitter cube splits the scattered light in its components, parallel and perpendicular to the scattering plane. The fluxes are recorded by two detectors having the same field of view. The vial is mounted on a rotational device; thus the incident light beam and the vial rotate together to change the phase angle in the 10° – 165° range. With such a configuration, the detection system remains in a fixed position, to minimize the optical misalignment that can occur when the experiment is extensively used. Before 2000, the detectors for PROGRA2-Vis were photodiodes but were replaced by CCD cameras after 2000. A third CCD camera is mounted on the rotational device to record the scattered light at a constant phase angle of 90° , which acts as a reference point to normalize the flux recorded by the 2 other cameras. This design allows to retrieve both polarization and brightness phase curves simultaneously. For PROGRA2-IR, only 2 cameras are used (no reference camera is present).

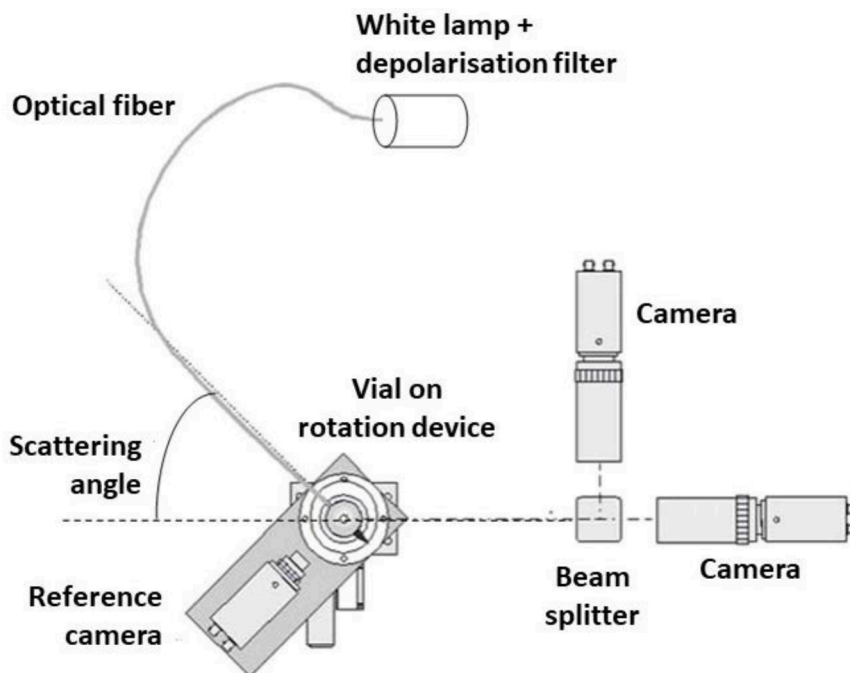


Fig. 1. Optical design and measurements with PROGRA2-VIS. For PROGRA2-IR, no reference camera is present.

because of some mechanical constraints), thus only the polarization curve can be retrieved. Such an imaging system allows rejecting the images for which the number density of particles is too large, producing thereby multiple scattering that can affect the accuracy of the analysis. Tests have been conducted to define an automatic image rejection criterion, based on the number of particles that are present in the field of view. The system is integrated inside an optical compartment that can be sealed to ensure that straylight is does not enter the device.

Levitation is produced by two different methods. The air draught method consists of creating a small airflow along the wall of the vial to gently lift the particles (usually smaller than about 20 μm). The particles are deposited initially on the bottom of the vial and levitate due to the airflow, for at least several seconds. When using submicron-sized particles or aggregates of submicron grains, the levitation can last several minutes. For largest particles, typically greater than 20 μm for dense grains and several tens of μm for aggregates, the levitation is obtained during parabolic flights onboard dedicated planes (Caravelle ZeroG, NASA KC-135, A300 ZeroG, A310 ZeroG, see Fig. 2a). These campaigns were managed by the Novespace company and were funded by the French space agency (CNES) and by the European space agency (ESA). During the 30 years of the project, PROGRA2 has participated in 67 campaigns and has undergone 6050 parabolas.

Microgravity conditions occur during each parabola, for which measurements are obtained at a fixed phase angle. Then, the phase angle is changed, typically by steps of 5° or 10°, and a new measurement is obtained during the next parabola. A phase curve can be described by 20 such points; thus 20 series of measurements are necessary per sample and per wavelength. Small concentrations of particles are necessary to produce optically thin media avoiding multiple scattering. However, a minimal number of particles is required to achieve statistically significant random orientations [20].

PROGRA2-Surf uses a different configuration for measurements performed in the laboratory (Fig. 2b). The sample is contained in a cup that is deposited on the plane surface. Both light source and detection system (cameras + beam splitter) can be rotated manually by steps of 5° and 10°. The measurements are usually obtained with a specular configuration, i.e. where the angles between the light source and the detectors are symmetrical with respect to the vertical direction. As with the other PROGRA2 instruments, the detectors are CCD cameras.

The flux scattered by the sample is recorded by the detectors at fixed phase angles. The polarized components I_1 and I_2 are the scattered flux perpendicular and parallel to the scattering plane, respectively. For PROGRA2-Vis, I_3 is the flux recorded by the reference camera. For the 3 versions of the experiment, the linear polarization P is calculated by:

$$P(\%) = 100 \times (I_1 - I_2) / (I_1 + I_2) \quad (1)$$

For PROGRA2-Vis, the brightness is calculated by:

$$B(\text{relative units}) = (I_1 + I_2) / I_3 \quad (2)$$

Such normalization prevents accurate retrieval of the brightness at the smallest and largest phase angles. For geometrical reasons, the field of view and the spatial resolution of the polarization cameras change when reaching extreme angles, while the field of view remains constant for the reference camera.

For PROGRA2-surf, since the particles do not move inside the cup during the measurement sessions, the brightness can be calculated by:

$$B(\text{relative units}) = (I_1 + I_2) \quad (3)$$

The error bars are derived by considering the number of particles detected and the amplitude of the scattered flux recorded by the polarization cameras, and standard deviation calculations. They are of the order of 1–2 % for measurements in the visible domain and of 5 % in the near infrared.

The size distribution for the levitating particles is established from the images, where the field of view was calibrated using a high-resolution graduated grid. Here we consider the equivalent diameter, which corresponds to the diameter of the particles if they were spherical. The observed size distribution can differ from the size distribution obtained by electron-microscopy in the laboratory, due to the formation of aggregates and agglomerates that can occur when the particles are lifted. During parabolic flights, the sample encounters 1.8 g periods before and after each parabola that provides microgravity conditions, when the plane is in the “pull-up” and “pull-out” phases. These hyper-gravity conditions can lead the particles to stick together at the bottom of the vial. When using the air draught technique, particles larger than 20 μm are also often observed, because of the aggregations processes that occur at the beginning of the lifting process.

Finally, sessions of validation to assess the measurements accuracy were performed after each improvement of the electronics and change of detectors, using calibrated glass beads of 100 μm [32–34].

3. The PROGRA2 database

The database is available in open access at: <https://www.icare.univ-lille.fr/progra2/>

The website is in English and in French. The instruments and the method of measurements are presented. 170 samples are available in the database, covering a large range of compact and fluffy particles with different compositions and with sizes, ranging from 10 nm for the constituent grains in aggregates to hundreds of μm for compact grains and aggregates. For some samples, the phase curves are given for different grain sizes. The samples under study can be grouped in different families (Table 1), and a significant part of the database concerns optically absorbing particles.

The database provides, when available, the description of the material, images by scanning electron or transmission microscopy to determine the shape and the size distribution of the particles on the ground, the conditions of measurements, the observed size distribution

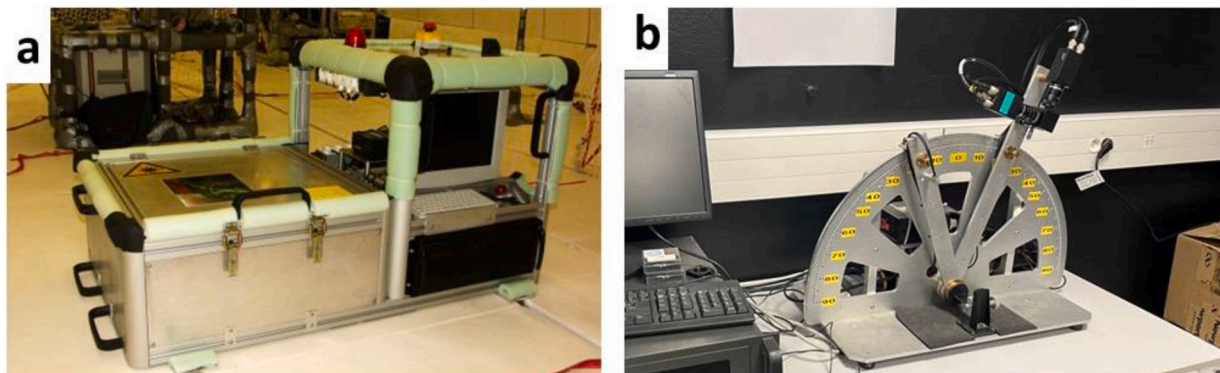


Fig. 2. a, PROGRA2-Vis inside the A300 ZeroG plane; b, PROGRA2-Surf.

Table 1
The different families of grains in the PROGRA2 database.

| Families | Material |
|-----------------|---|
| Analog | Comets, interplanetary dust, Mars, Moon, Titan |
| Asbestos | Actinolite, amosite, antigorite, chrysotile, crocidolite |
| Ashes | Industrial, volcano (Eyjafjallajökull, Etna, Lokon,) |
| Beads and cubes | Glass, silica, rounded cubes |
| Carbonaceous | Carbon black, coal (anthracite, charcoal, kerite, lignite), diamond, graphite |
| Dusty plasmas | Spheres, tholins (spherical grains and needles) |
| Iron compounds | Iron-silica, Iron-sulfide |
| Meteorites | Allegan, Allende, Aubrite, Orgueil, North West Africa 6352 and 6445 |
| Minerals | Alumina, basalt, boron carbide, cement, clay, loess, pyrrhotite, pumice stone, silica, silicates, silicon carbide, titanium oxide |
| Pollens | Grass: barley, corn, couch grass, fescue orchard grass, timothy grass, velvet grass, vernal grass, wheat Weed: mugwort, plantain, ragweed, wall pellitory Tree: alder, ash, birch, cypress, fir, hazel olive tree, plane tree |
| Sand | Grains from different locations, quartz |
| Salts | Potassium bromide, potassium chloride, sodium chloride |
| Silicates | AlSiO ₃ , MgSiO ₃ , FeSiO ₃ , enstatite, forsterite, garnet, olivine, pyroxene, quartz |
| Soot | Ethylene, kerosene, PMMA, propane, toluene |

in the clouds, and the polarization and brightness curves at the different wavelengths. The experimental results are presented in the form of figures and tables that can be downloaded.

The description of the conditions of measurements indicates if the results were obtained for particles levitated during microgravity conditions or by an air draught. These different conditions impact the size distributions, and thus the polarization and brightness curves, when they depend on the particles' size.

Fig. 3 presents an example of the results for the Lokon volcanic ashes, available at the 4 wavelengths, from measurements carried out in microgravity. Fig. 4 presents the results for aggregates of 14 nm monomers of carbon black, available in the visible domain, from measurements using the air draught method.

The phase curves were obtained by integrating the contribution of all levitating particles detected by the cameras. On the other hand, the imaging system also allows us to retrieve the individual particles' contribution for measurements in the 40°–140° range and for particles larger than about 50 µm. It is therefore possible to retrieve the evolution of the polarization and brightness values with size. Such results are not provided in the database since they need specific reprocessing but can be processed upon request to the authors.

4. Main results already obtained from the PROGRA2 database

4.1. Context

Light scattering by irregular particles depends on various characteristics of the particles: global shape, irregularities (facets, angles), materials (transparency, absorption), coating by a second material, size of the particle, and size of their constituent grains. The size of each particle in the field of view is measured on the polarization images. The original size of the grains in the samples are measured on SEM or TEM images before the particles are introduced in the vial.

The main parameters to compare laboratory phase curves to remote sensing curves are the maximum polarization P_{\max} and the minimum polarization P_{\min} , their corresponding phase angles α_{\max} and α_{\min} , the inversion angle α_0 (where the sign of the polarization changes), and the slope at inversion h . Such curves can also be compared to input numerical simulations to improve the modelling approach for irregular grains. The polarization often provides easier interpretations than the brightness since the difference from one sample to another may be made more obvious, although the brightness phase curves can provide

information on the structure of the particles.

4.2. Differences between lifted and deposited particles in layers

The first purpose of PROGRA2 was to compare the polarization and brightness phase curves for similar samples lifted in clouds and deposited in layers on a surface. Different samples were used and the characteristics of the curves were compared [35]. To illustrate the differences, the maximum amplitude of the polarization curve P_{\max} at a phase angle α_{\max} was often considered. P_{\max} values can strongly differ depending on the materials and their refractive indices, on the size of the particles and on the size of their constituent grains in aggregates. Large particles are more optically absorbing than smaller ones and P_{\max} is usually higher then. Single scattering should only be considered for clouds of particles when the media is optically thin. In case of layers, multiple scattering between the particles may occur. When the absorption increases, the multiple scattering decreases and P_{\max} may be similar for lifted small aggregates and large deposited ones [36]. Between lifted and deposited particles α_{\max} may also be different, usually closer to 90° for lifted particles and larger for layers, mainly when the particles are large and transparent (up to hundreds of micrometers). When the media is optically thick, as for dense clouds or deposited particles, the value of P_{\max} also depends on the number density of the particles.

4.3. Relation between the phase curves and the physical properties of the particles

Systematic studies [37–40] were conducted for the evolution of polarization with size for lifted and deposited particles in the [1–500] µm size range. The particles can be almost transparent (like silica and quartz), very absorbing (like carbon and coal), compact, or fluffy aggregates with porosity as high as 90 % and made of constituent grains in the [10–100] nm size range.

For all kinds of samples, the variation of P_{\max} as a function of size of the grains is similar. When the size of the grains increases from 10 nm up to 100 nm, P_{\max} decreases independently of the absorption. For sizes of the grains larger than the wavelength, P_{\max} increases. The limit between the two regimes depends on the absorption (imaginary part of the refractive index).

For compact particles or aggregates, when the size of large particles increases, P_{\max} increases up to a limit when all the light that enters the particle is absorbed (sometimes called saturation effect); then only the external surface or the external grains reflects the light. If multiple scattering occurs, it will be produced by the surface of the particles only.

Other studies concern mixtures of carbon-black with silica/silicates fluffy aggregates in different ratios and for different sizes of the constituent grains (with an average size of 40 nm for each mixture). The resulting polarization curve mainly depends on the average size of the grains and on the albedo of the mixtures [39,40]. The albedo depends on the refractive indices, the sizes of the monomers, but also on the structure of the aggregates. Indeed, size and albedo are strongly correlated, and disentangling their effect needs experimental works confirmed by numerical simulations. Nevertheless, the main parameter remains the size of the constituent grains in aggregates, the size of the fluffy particles having a smaller effect, independently of the chemical composition. When the average size of the grains increases, P_{\max} decreases. A similar effect is observed when compact µm-sized silica particles are added to the fluffy mixtures.

The mixture of carbon black with Mg-SiO and Fe-SiO samples [39, 40] having different shapes for the grains and the structure of the aggregates can be used to study the influence of the wavelength on the P_{\max} values. Except for Fe-SiO, the spectral gradient is positive for all single materials and for their mixtures. If 50 % of C-black is added to 50 % of Fe-SiO, the spectral gradient is again positive, showing the influence of carbonaceous materials. Also, the negative branch ($P < 0$) of the phase curves exists for all the mixtures, probably because of different

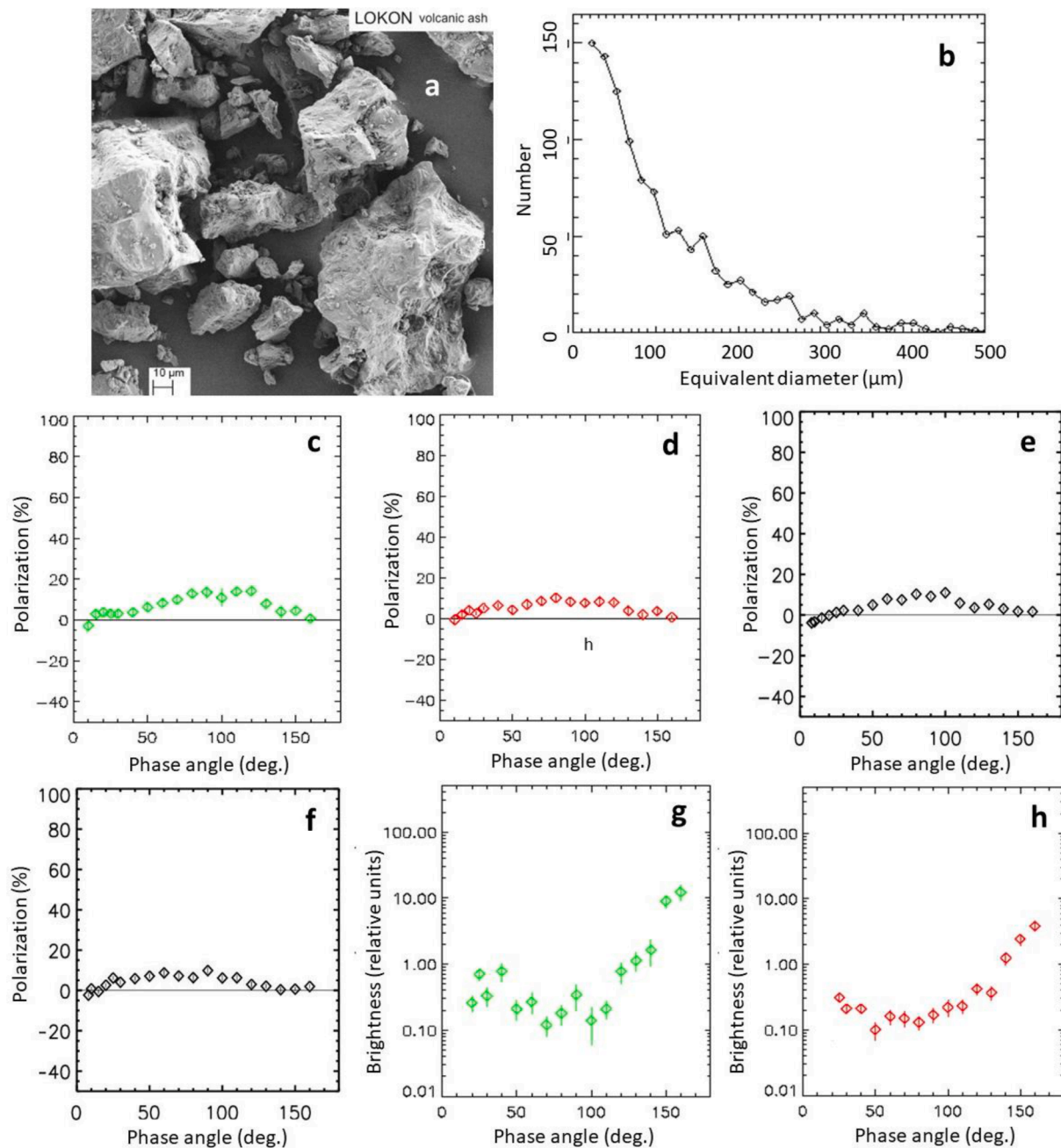


Fig. 3. Figures for the Lokon (volcanic ashes) sample; the measurements were obtained in microgravity during parabolic flights. a: scanning electron microscope image, b: size distribution for levitating particles; c: linear polarization curve at 540 nm; d: linear polarization curve at 640 nm; e: linear polarization curve at 950 nm; f: linear polarization curve at 1500 nm; g: brightness curve at 540 nm; h: brightness curve at 640 nm.

size distributions of the grains and different albedo. All these studies can be used to choose samples that are considered as representative of cometary particles.

Some intriguing results are found between the polarization for layers and clouds of partly transparent sands with large grains of different colors. P_{\max} for layers is systematically higher for large deposited particles than for clouds independently of the materials. Conversely, for layers of small particles in the [5–10] μm range, the usual trend is found, with a decrease of P_{\max} by multiple scattering for the layers. Both large and small particles were detected when lifted, although the surface of the layers seem to be mainly formed by the largest grains hiding the smaller ones, phenomenon known as Brazil nuts effect [41], thus producing higher polarization values.

The scattering properties of the particles depend on their size relative

to the wavelength, thus the size parameter of the particles must be considered (the size parameter is equal to $2\pi R/\lambda$ where R is the radius of the particles and λ wavelength of the observation). If the refractive index is constant at the studied wavelengths, the differences between the polarization phase curves are due only to the differences in the size parameter. If the refractive index changes with the wavelength, then the differences between the phase curves have to be analyzed in detail to interpret them (an example is given below for tholins). For aggregated particles composed of submicron monomers, the size parameter of the monomer must also be considered. Fig. 5a presents the wavelength effect for the carbon black. When considering the size parameter of the monomers, the evolution of maximum polarization with size becomes almost similar in the visible domain (Fig. 5b), although some differences remain in the near-infrared domain, where the effect of the refractive

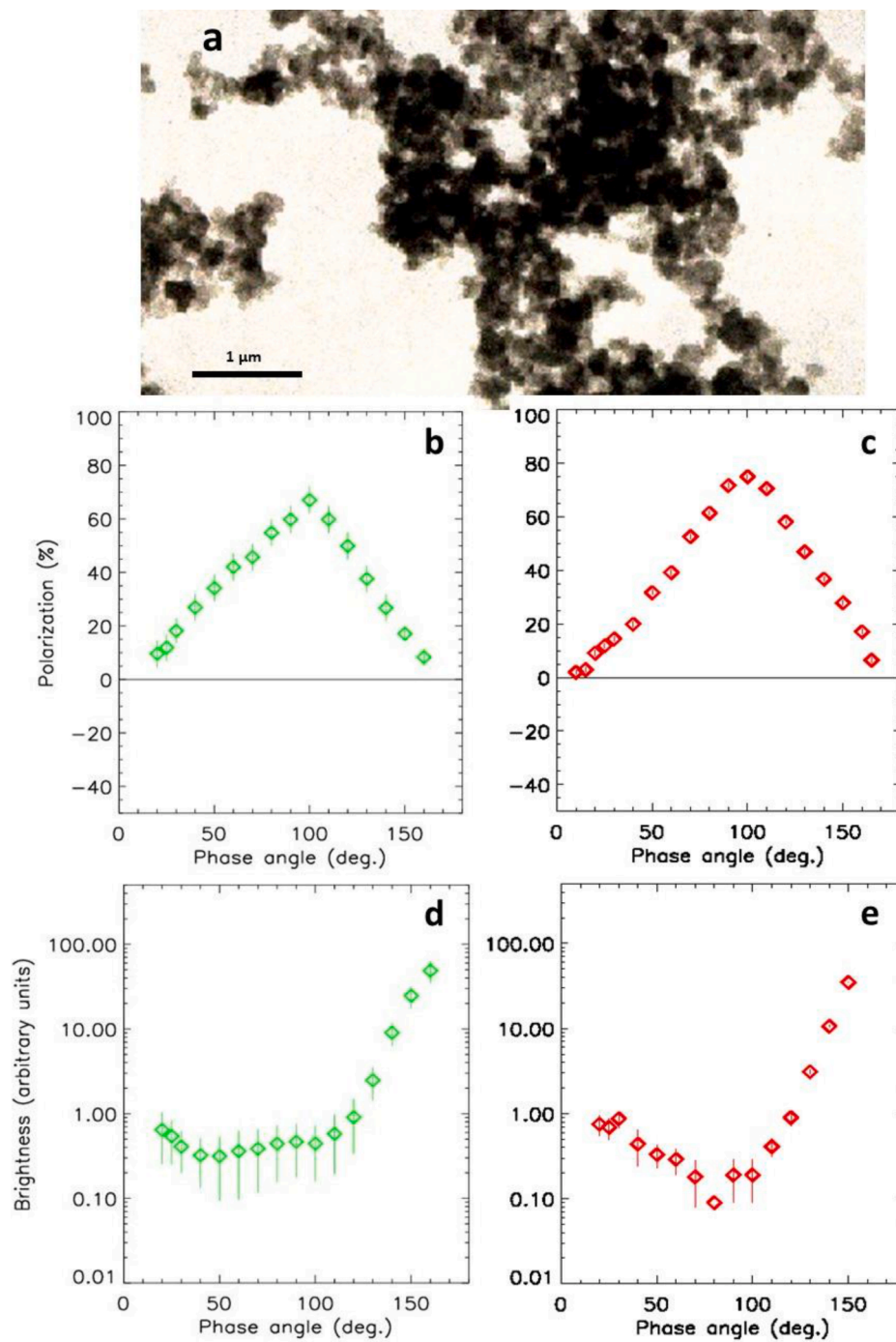


Fig. 4. Figures for the aggregates of 14-nm monomers of carbon black sample; the measurements were obtained using the air draught technique. a: transmission electron microscope image; b: linear polarization curve at 540 nm; c: linear polarization curve at 640 nm; d: brightness curve at 540 nm; e: brightness curve at 640 nm.

index variability should occur.

The variation of polarization as a function of wavelength for powdered meteorite Allende with compact grain's size in the [42-500] μm range is of interest when compared to cometary observations. P_{max} increases from green to red to a maximum value for a wavelength of 1000 nm and finally decreases at 1500 nm (Fig. 6). This variation is the same as that observed for some comets like Hale-Bopp [5]. This variation of polarization could be attributed to variations of refractive index related to the chemical composition of the sample and its spectroscopy properties.

Dusty plasmas (tholins) can be given as an example of the link

between physical properties of the particles and the phase curves for particles in the same family. Tholins can be produced from different ratios of CH_4/N_2 [43]. As the CH_4/N_2 ratio decreases, the color becomes clearer (the absorption is decreasing), the diameter of the grains increases, and the composition changes with an increasing content of amine. Such changes significantly affect the phase curves: P_{max} decreases when the size of the constituent grains in the aggregates increases (but remains smaller than the wavelength), P_{min} increases when the absorption decreases, and the value of the α_0 angle increases for decreasing CH_4/N_2 ratios.

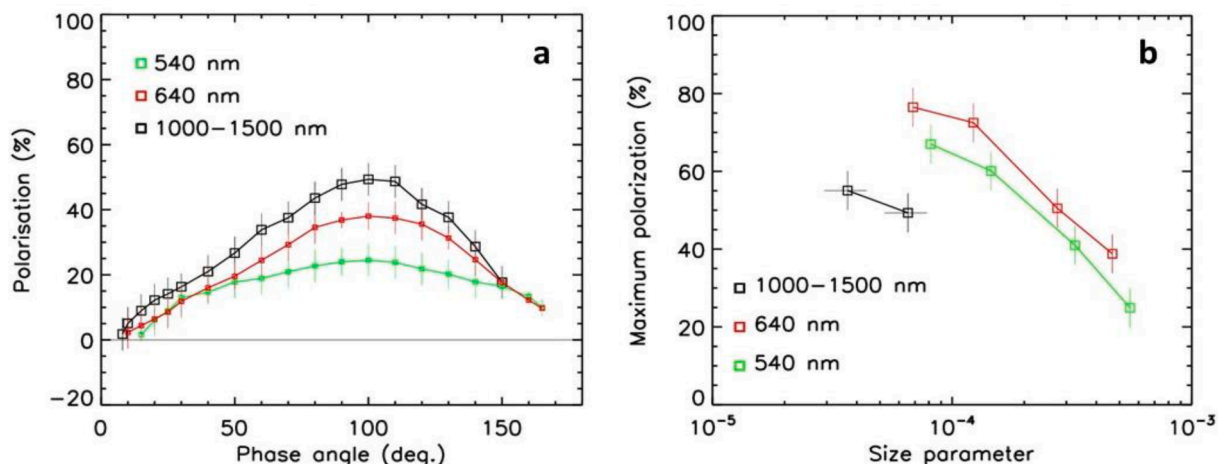


Fig. 5. Linear polarization curves for black carbon. a: Polarization curves at 3 wavelengths for aggregates of carbon black with monomers of 95 nm. b: Evolution of the maximum polarization with the size parameter of the monomers and the wavelength.

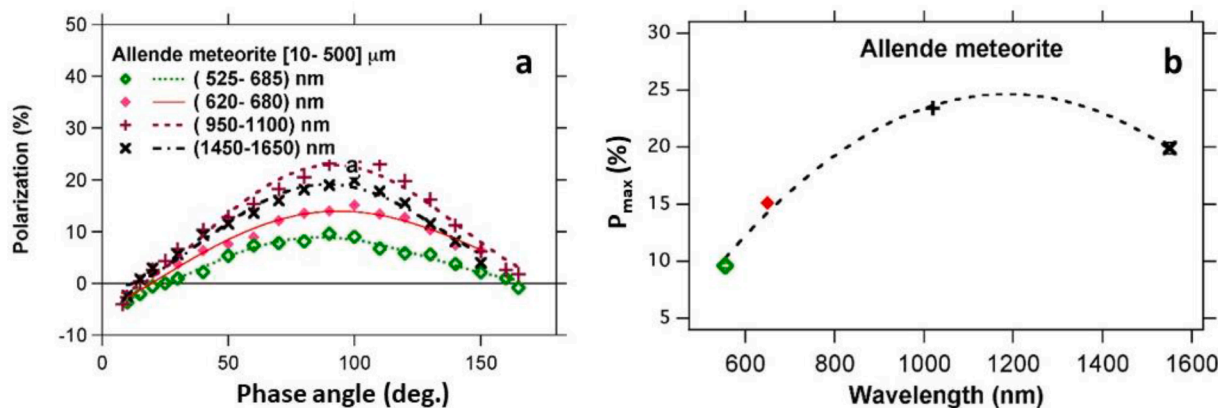


Fig. 6. Evolution of the polarization with wavelength for powered meteorite Allende; a: phase curves; b: evolution of P_{max} with wavelength.

4.4. Experimental and numerical models for particles with different shapes and structures

Several modelling approaches have been developed to successfully reproduce some of the polarization curves of the PROGRA2 database. SiO_2 μm -sized spheres were used to study the evolution of the scattering properties from individual spherical monomers to high porosity aggregates and to densely packed layers [30,44].

The presence of coating on glass and silica spheres shows that a thin layer of optically-absorbing mantle can significantly change the polarization curves [45]. On the opposite a transparent coating, such as ice mantles on the particles, appears to be very difficult to detect.

Finally, ray-tracing methods were used to model the optical properties of rounded salt cubes of several hundred of μm [46] and for B_4C compact grains of several tens of μm having sharp edges. The experiment allowed estimating the complex refractive index of the material [47].

4.5. Analogs of dust in some objects of the solar system

The 4 main parameters previously mentioned, P_{max} , α_{max} , α_0 and h , are used for the comparison of remote sensing measurements with laboratory analogs of dust in the solar system. The α_0 angle and the zone where the polarization values are negative (at small phase angles), indicate a change in the direction of polarization [48–50]. However, such values are not always considered when the PROGRA2 accuracy is of the order of the polarization values.

The main results for some analogs of solar system dust are given below.

4.5.1. Lunar, Martian and asteroids analogs

The NASA JSC1 analogs of materials for the Lunar or Martian surfaces yield phase curves that are close to those obtained from remote sensing measurements, giving confidence on the quality of the analog for the main composition and size distribution [35].

Analogues for asteroids are tested by using powdered meteorites that are supposed to be fragments from the asteroids. The samples are currently first sifted in the laboratory to control the size distribution. Compared to phase curves for asteroids, the laboratory measurements give some indication on the size and the composition and albedo of the particles. Considering both lifted particles with very high porosity and very absorbing materials that have similar phase curves in levitation and in layers, the Orgueil meteorite low density aggregates formed in microgravity can be considered as a good analog to confirm the presence of the mm-sized to cm-sized particles at the surface of the dark Near-Earth asteroids [42].

4.5.2. Analogs for cometary dust in the coma

Some questions for the properties of dust particles in comets remain open. The in-situ observations (as obtained by Rosetta on comet 67P) give some important answers but space missions are rare and are at present limited to periodic comets. Remote observations are necessary to study a large number of comets with different dust properties and the

inhomogeneous optical properties in their coma. Discrepancies are noticed on the polarization phase curves mainly in the P_{\max} region [5, 51]. The composition of the dust from Rosetta measurements gives a ratio of minerals on C-compounds of about 50 %, with a mixture of aggregates of different compactions, from very fluffy fractal types to compact ones. Irregular particles 100 μm -sized were observed with constituent grains having size down to 10 nm [52].

The analogs used in the PROGRA2 experiment are composed of different mixtures of silicates with various structures (fluffy and compact), compositions and colors, and of carbon black and coal particles. Such mixtures are necessary to reproduce the different polarization phase curves obtained from remote sensing observations and Rosetta measurements, and the typical “U-shape” brightness phase curve obtained for 67P/Rosetta observations [53].

4.5.3. Interplanetary dust analogs in the symmetry plane

For the interplanetary dust, the decrease of the maximum polarization with decreasing distance to the Sun can be explained by a decrease of the percentage of organic materials compared to silicate materials, as proposed from numerical simulations [8]. The various samples studied with PROGRA2, where such percentages varied, successfully reproduced the results of the polarization change with distance to the Sun [54].

4.5.4. Titan's aerosols analogs

The aerosols of the Titan atmosphere can be reproduced in laboratory by tholins particles produced by the PAMPRE experiment [55]. The variation of the methane-nitrogen mixture composition and the duration of radio frequency discharge change the color and the size of the monomers and their composition. Aggregates of monomers smaller than 90 nm reproduce very well the remote sensing measurements from spacecraft [43].

4.6. Solid particles in the Earth atmosphere

Although liquid sulfate particles are the main component of aerosols in the Earth stratosphere, some solid particles coming from space, from volcanos, from biomass burning and from anthropogenic pollution, were detected [56]. The in-situ brightness curves obtained from balloon-borne measurements compared to the laboratory measurements of carbonaceous particles indicate that mixtures of soot and liquid sulfate are present up to the middle stratosphere, and that soot could be the main component of submicron particles [12] at some altitudes.

The specific optical properties of some families of atmospheric particles were studied with PROGRA2 to develop new instruments. The brightness curves of pollens often differ from those of non-biological particles [57]. Thus, specific scattering angles have been chosen to determine the particle concentrations and to be able to discriminate the various pollens families in ambient air. This is the purpose of the Beemose instrument [58] now produced by the Lify-Air Company. Also, some of the asbestos particles exhibit specific brightness phase curves; in particular, the chrysotile brightness curve presents a decreasing amplitude close to 3 orders between 15° and 90° scattering angle, because of the tubular shape of the particles that can act as a light trap [59]. A possible new instrument is still in development for the detection of asbestos in a container from crushed building materials.

5. Conclusions

The large number of studied samples at 4 wavelengths for levitated and deposited particles, covering the main natures and families of particles that can be found in space and in planetary atmospheres, can be used as a reference database to interpret remote sensing scattering measurements by clouds and surfaces of irregular particles. The techniques of levitation ensure that the particles are randomly oriented, to be able to use the statistical approach that is necessary to retrieve the mean brightness and linear polarization curves.

Numerous applications were already conducted to better determine some physical properties of dust in comets, in interplanetary medium, on asteroids' surface, in Titan atmospheres, and for some particles in the Earth atmosphere. Another application of the PROGRA2 heritage is involved in the ICAPS project, funded by ESA, dedicated to the study of the agglomeration process in microgravity conditions [60,61]. As part of the instrumentation, the Light Scattering Unit has been developed to perform measurements at 3 different phase angles to follow the evolution of the brightness and polarization curves during the aggregation processes. A flight under a ballistic Texus rocket successfully occurred in April 2023.

All these results and projects plead for future space-borne instrumentation for in situ measurements to retrieve locally on board a descending probe, a balloon or a drone, the phase curves of the particles in space and in planetary atmospheres to better characterize them [62]. Although the PROGRA2 project ended in 2022, meaning that no new measurements will be obtained with these instruments, new generations of instruments are in development and start to be used, as the laboratory spectro-gonio radiometer SHADOWS instrument that can perform measurements between 350 nm to 4800 nm [63]. The measurements are obtained at present for deposited particles, but a new version will measure in the near future levitating particles, using the air draught technique. Such instrumentation can also be used to better evaluate the wavelength dependence of the refractive index of the particles.

In addition to spectroscopic measurements that provide information on the composition of the solid particles, the analysis of the scattered light can provide useful information on the size, the shape and the refractive index of such particles in clouds, and the PROGRA2 project has made a significant contribution on this topic.

CRedit authorship contribution statement

Jean-Baptiste Renard: Writing – original draft, Visualization, Supervision, Software, Resources, Project administration, Methodology, Investigation, Funding acquisition, Formal analysis, Data curation, Conceptualization. **E. Hadamcik:** Writing – review & editing, Validation, Methodology, Investigation, Formal analysis, Conceptualization. **J.-C. Worms:** Writing – review & editing, Resources, Project administration, Conceptualization.

Declaration of competing interest

The authors declare that they have no known competing financial interests or personal relationships that could have appeared to influence the work reported in this paper.

Data availability

Data will be made available on request.

Acknowledgments

This paper is in memory of Prof. Anny-Chantal Levasseur-Regourd who was one of the founders of the project. The authors want to thank all the colleagues, the technical teams and the students who have participated in the PROGRA2 project, Djamel Loualia (AERIS/ICARE) for the website, the space agency CNES and ESA for their 30 year support, and the Novespace company for the parabolic flights.

References

- [1] Hapke B. Theory of reflectance and emittance spectroscopy. Topics in remote sensing, 3. Cambridge: Cambridge University Press; 1993.
- [2] Hovenier JW. Measuring scattering matrices of small particles at optical wavelengths. In: Mishchenko MI, Hovenier JW, Travis LD, editors. Light scattering by nonspherical particles. San-Diego: Academic Press; 2000. p. 355–65.

- [3] Levasseur-Regourd AC, Hadamcik E, Renard JB. Evidence for two classes of comets from their polarimetric properties at large phase angle. *Astron Astrophys* 1996; 313:327–33.
- [4] Bertini I, La Forgia F, Tubiana C, Güttler C, Fulle M, Moreno F, et al. The scattering phase function of comet 67P/Churyumov–Gerasimenko coma as seen from the Rosetta/OSIRIS instrument. *MNRAS* 2017;469. <https://doi.org/10.1093/mnras/stx1850>. S2:S404–15.
- [5] Hadamcik E, Levasseur-Regourd AC. Dust evolution of comet C/1995 O1 (Hale-Bopp) by imaging polarimetric observations. *Astron Astrophys* 2003;403:757–68. <https://doi.org/10.1051/0004-6361:20030378>.
- [6] Bagnulo S, Cellino A, Kolokolova L, Bagnulo S, Nežić R, Santana-Ros T, Borisov G, Christou AA, Bendjoya P, Devogèle M. Unusual polarimetric properties for interstellar comet 2I/Borisov. *Nat Commun* 2021;12:1797. <https://doi.org/10.1038/s41467-021-22000-x>.
- [7] Dumont R, Levasseur-Regourd AC. Zodiacal light gathered along the line of sight, retrieval of local scattering coefficient from photometric surveys of the ecliptic plane. *Planet Space Sci* 1985;33:1–9.
- [8] Lasue J, Levasseur-Regourd AC, Renard JB. Zodiacal light observations and its link with cosmic dust: a review. *Planet Space Sci* 2020;190:104973. <https://doi.org/10.1016/j.pss.2020.104973>.
- [9] Levasseur-Regourd AC, Dumont R, Renard JB. A comparison between polarimetric properties of cometary dust and interplanetary dust particles. *Icarus* 1990;86: 264–72. [https://doi.org/10.1016/0019-1035\(90\)90215-U](https://doi.org/10.1016/0019-1035(90)90215-U).
- [10] Tomasko MG, Dooze L, Dafee LE, See C. Limits on the size of aerosols from measurements of linear polarization in Titan's atmosphere. *Icarus* 2009;204: 271–83.
- [11] West RA, Hart H, Simmons KE, Hord CW, Esposito LW, Lane AL, Pomphrey RB, Coffeen DL, Sato M. Voyager 2 photopolarimeter observations of Titan. *J Geophys Res Space Phys* 1983;88:8699–708. <https://doi.org/10.1029/JA088iA11p08699>.
- [12] Renard JB, Brogniez C, Berthet G, Bourgeois Q, Gaubicher B, Chartier M, Balois JY, Verwaerde C, Auriol F, Francois P, Daugeron D, Engrand C. Vertical distribution of the different types of aerosols in the stratosphere, detection of solid particles and analysis of their spatial variability. *J Geophys Res* 2008;113:D21303.
- [13] Esposito TM, Duchêne G, Kalas P, et al. Direct imaging of the HD 35841 debris disk: a polarized dust ring from Gemini Planet Imager and an outer halo from HST/STIS. *Astron J* 2018;156:47. <https://doi.org/10.3847/1538-3881/aabc9>.
- [14] Graham JR, Kalas P, Matthews B. The signature of primordial grain growth in the polarized light of the AU Microscopii debris disk. *Atrophys J* 2007;654:595–605. <https://doi.org/10.1086/509318>.
- [15] Milli J, Engler N, Schmid HM, et al. Optical polarised phase function of the HR 4796a dust ring. *Astron Astrophys* 2019;626:A54. <https://doi.org/10.1051/0004-6361/201935363>.
- [16] Goidet B, Renard JB, Levasseur-Regourd AC. Polarization of asteroids, synthetic curves and characteristic parameters. *Planet Space Sci* 1995;43:779–86.
- [17] Hadamcik E, Levasseur-Regourd AC, Renard JB, Lasue J, Sen AK. Polarimetric observations and laboratory simulations of asteroidal surfaces: the case of 21 Lutetia. *JQSRT* 2011;112:1881–90.
- [18] Cellino A, Bagnulo S, Gil-Hutton R, Tanga P, Canada-Assandri M, Tedesco EF. A polarimetric study of asteroids: fitting phase–polarization curves. *MNRAS* 2016; 455:2091–100. <https://doi.org/10.1093/mnras/stv2445>.
- [19] Shkuratov YG, Opanasenko NV. Polarimetric and photometric properties of the moon: telescope observation and laboratory simulation: 2. The positive polarization. *Icarus* 1992;99(2):468–84.
- [20] Renard JB, Geffrin JM, Tobon Valencia V, Torteil H, Ménard F, Rannou P, Milli J, Berthet G. Number of independent measurements required to obtain reliable mean scattering properties of irregular particles having a small size parameter, using microwave analogy measurements. *JQSRT* 2021;272:107718. <https://doi.org/10.1016/j.jqsrt.2021.107718>.
- [21] West RA, Dooze LR, Eibl AM, Tomasko MG, Mishchenko MI. Laboratory measurements of mineral dust scattering phase function and linear polarization. *J Geophys Res* 1997;102(16):871–81.
- [22] Muñoz O, Hovenier JW. Laboratory measurements of single light scattering by ensembles of randomly oriented small irregular particles in air, a review. *JQSRT* 2011;112:1646–57.
- [23] Volten H, Muñoz O, Rol E, de Haan JF, Vassen W, Hovenier JW. Scattering matrices of mineral aerosol particles at 441.6 and 632.8nm. *J. Geophys. Res.* 2001;106 (D15):17375–401.
- [24] Muñoz O, Moreno F, Guirado D, Dabrowska DD, Volten H, Hovenier JW. The Amsterdam-granada light scattering database. *JQSRT* 2012;113(7):564–74.
- [25] Shkuratov Y, Ovcharenko A, Zubko E, Volten H, Munoz O, Videen G. The negative polarization of light scattered from particulate surfaces and of independently scattering particles. *JQSRT* 2004;88:267–84.
- [26] Shkuratov Y, Bondarenko S, Ovcharenko A, Pieters C, Hiroi T, Volten H, Muñoz O, Videen G. Comparative studies of the reflectance and degree of linear polarization of particulate surfaces and independently scattering particles. *JQSRT* 2006;100 (1–3). 340–58.
- [27] Shkuratov Y, Bondarenko S, Kaydash V, Videen G, Muñoz O, Volte H. Photometry and polarimetry of particulate surfaces and aerosol particles over a wide range of phase angles. *JQSRT* 2007;106(1–3). 487–08.
- [28] Daugeron D, Renard JB, Gaubicher B, Couté B, Hadamcik E, Gensdarmes F, Basso G, Fournier C. Scattering properties of sands, 1. Comparison between different techniques of measurements. *Appl Opt* 2006;45:8331–7.
- [29] Hadamcik E, Renard JB, Worms JC, Levasseur-Regourd AC, Masson M. Polarization of light scattered by fluffy particles (PROGRA2 experiment). *Icarus* 2002;155: 497–508.
- [30] Hadamcik E, Renard JB, Levasseur-Regourd AC, Lasue J, Alcouffe G, Francis M. Light scattering by agglomerates: interconnecting size and absorption effects (PROGRA2 experiment). *JQSRT* 2009. 110/1755–70.
- [31] Worms JC, Renard JB, Hadamcik E, Levasseur-Regourd AC, Gayet JF. Results of the PROGRA2 experiment: an experimental study in microgravity of scattered polarised light by dust particles with large size parameter. *Icarus* 1999;142: 281–97.
- [32] Worms JC, Renard JB, Levasseur-Regourd AC, Hadamcik E. Light scattering by dust particles in microgravity: the PROGRA2 achievements and results. *Adv. Space Res* 1999;23(7):1257–66.
- [33] Hadamcik E, Renard JB, Levasseur-Regourd AC, Worms JC. Laboratory light scattering measurements on « natural » particles with the PROGRA2 experiment: an overview. *JQSRT* 2003;79–80:679–93.
- [34] Renard JB, Hadamcik E, Couté B, Jeannot M, Levasseur-Regourd AC. Wavelength dependence of linear polarization in the visible and near infrared domain for large levitating grains (PROGRA2 instruments). *JQSRT* 2014;146:424–30.
- [35] Worms JC, Renard JB, Hadamcik E, Brun-Huret N, Levasseur-Regourd AC. Light scattering by dust particles with the PROGRA2 instrument - Comparative measurements between clouds under microgravity and layers on the ground. *Planet Space Sci* 2000;48. 493–05.
- [36] Hadamcik E, Renard JB, Lasue J, Levasseur-Regourd AC, Blum J, Shraepel R. Light scattering by low density agglomerates of micron-sized grains with the PROGRA2 experiment. *JQSRT* 2007;106:74–89.
- [37] Renard JB, Francis M, Hadamcik E, Daugeron D, Couté B, Gaubicher B, Jeannot M. Scattering properties of sand. 2. Results for sands from different origins. *Appl Opt* 2010;49(18):3552–9.
- [38] Francis M, Renard JB, Hadamcik E, Couté B, Gaubicher B, Jeannot B. New studies on scattering properties of different kinds of soot. *JQSRT* 2011;112:1766–75.
- [39] Hadamcik E, Renard JB, Levasseur-Regourd AC, Lasue J. Light scattering by fluffy particles with the PROGRA2 experiment: mixtures of materials. *JQSRT* 2006;100: 143–56.
- [40] Hadamcik E, Renard JB, Rietmeijer FJM, Levasseur-Regourd AC, Hill HGM, Karner JM, Nuth JA. Light scattering by fluffy Mg-Fe-SiO and C mixtures as cometary analogs (PROGRA2 experiment). *Icarus* 2007;190:660–71.
- [41] Rosato A, Strandburg KJ, Prinz F, Swendsen RH. Why the Brazil nuts are on top: size segregation of particulate matter by shaking. *Phys Rev Lett* 1987;58:1038.
- [42] Hadamcik E, Renard JB, Lasue J, Levasseur-Regourd AC, Ishiguro M. Low-albedo asteroids: analogues with a high polarization at large phase angles. *MNRAS* 2023; 520:1963–74.
- [43] Hadamcik E, Renard JB, Majhoub A, Gautier T, Carrasco N, Cernogora G, Szopa C. Optical properties of analogs of Titan's aerosols produced by dusty plasmas. *Earth Plan Space* 2013;65:1175–84.
- [44] Väisänen T, Markkanen J, Hadamcik E, Renard JB, Lasue J, Levasseur-Regourd AC, Blum J, Muinonen K. Scattering of light by a large, densely-packed agglomerate of small silica spheres. *Opt Lett* 2020;45(7):1679–82.
- [45] Lasue J, Levasseur-Regourd AC, Hadamcik E, Renard JB. Light scattering by coated spheres: experimental results and numerical simulations. *JQSRT* 2007;106:212–24.
- [46] Mikrenska M, Koulev P, Renard JB, Hadamcik E, Worms JC. Direct simulation Monte Carlo ray-tracing model of light scattering by a class of real particles and comparison with PROGRA² experimental results. *JQSRT* 2006;100:256–67.
- [47] Penttilä A, Lumme K, Worms JC, Hadamcik E, Renard JB, Levasseur-Regourd AC. Theoretical analysis of the particles' properties and polarization measurements in the PROGRA2 experiment. *JQSRT* 2003;79–80. 1043–49.
- [48] Frattin E, Munoz O, Moreno F, Nava J, Escobar-Cerezo J, Gomez Martin JC, Guirado D, Cellino A, Coll P, Raulin F, Bertini I, Cremonese G, Lazzarin M, Naletto G, La Forgia F. Experimental phase function and degree of linear polarization of cometary dust analogues. *MNRAS* 2019;484:2198–211.
- [49] Muinonen KO, Sihvola AH, Lindell IV, Lumme KA. Scattering by a small object close to an interface II. Study of backscattering. *J Opt Soc Am* 1991;A8:477–82.
- [50] Zubko E. Interpretation of similarity in the negative polarization of comets and C-type asteroids in terms of common properties of asteroidal and cometary dust. *Earth Plan Spa* 2011;63:1077–85.
- [51] Hadamcik E, Levasseur-Regourd AC. Imaging of cometary dust: different comets and phase angles. *JQSRT* 2003;79(80):661.
- [52] Mannel T, Bentley MS, Boakes PD, Jeszenszky H, Ehrenfreund P, Engrand C, Koebel C, Levasseur-Regourd AC, Romstedt J, Schmied R, Torkar K, Weber I. Dust of comet 67P/Churyumov-Gerasimenko collected by Rosetta/MIDAS: classification and extension to the nanometer scale. *Astron Astrophys* 2019;630:A26.
- [53] Levasseur-Regourd AC, Renard JB, Hadamcik E, Lasue J, Bertini I, Fulle M. Interpretation through experimental simulations of phase functions revealed by Rosetta in 67P dust com. *A&A* 2019;630:A20.
- [54] Hadamcik E, Lasue J, Levasseur-Regourd AC, Renard JB. Analogues of interplanetary dust particles to interpret the zodiacal light polarization. *Planet Space Sci* 2020;183:104527.
- [55] Szopa C, Cernogora G, Boufendi L, Correia JJ, Coll P. PAMPRE a dusty plasma experiment for Titans tholins production and study. *Planet Space Sci* 2006;54: 394–404.
- [56] Renard JB, Berthet G, Levasseur-Regourd AC, Beresnev S, Miffre A, Rairoux P, Vignelles D, Jégou F. Origins and spatial distribution of Non-Pure Sulfate Particles (NSPs) in the stratosphere detected by the balloon-borne Light Optical Aerosols Counter (LOAC). *Atmosphere (Basel)* 2020;11:1031.
- [57] Renard JB, El Azari H, Richard J, Lauthier J, Surcin J. Towards an automatic pollen detection system in ambient air using phase functions in the visible domain. *Sensors* 2022;22:4984.

- [58] El Azari H, Renard JB, Lauthier J, Dudok de Witt T. A laboratory evaluation of the new automated pollen sensor Beenose: pollen discrimination using machine learning technique. *Sensors* 2023;23:2964.
- [59] Renard JB, Duée C, Bourrat X, Haas H, Surcin J, Couté B. Brightness and polarization phase functions of different natures of asbestos in the visible and near infrared domain. *JQSRT* 2020;253:107159.
- [60] Poppe T, Blum J, Henning T. Experiments on dust aggregation and their relevance to space missions. *Adv Spac Res* 2022;29(5):763–71.
- [61] Schubert B, Molinski N, Blum J, Glißmann T, Pöppelwerth A, von Borstel I, Balapanov D, Vedernikov A, Houge A, Krijt S. ICAPS: dust aggregate properties and growth derived from Brownian translation and rotation from the ballistic to the diffusive limit. *EPSC* 2022;581:18–23.
- [62] Renard JB, Mousis O, Rannou P, Levasseur-Regourd AC, Berthet G, Geffrin JM, Hadamcik E, Verdier N, Millet AL, Daugeron E. Counting and phase function measurements with the LONSCAPE instrument to determine physical properties of aerosols in ice giant planet atmospheres. *Space Sci Rev* 2020;206:28.
- [63] Potin S, Brissaud O, Beck P, Schmitt B, Magnard Y, Correia JJ, Rabou P, Jocou L. SHADOWS: a spectro-gonio radiometer for bidirectional reflectance studies of dark meteorites and terrestrial analogs: design, calibrations, and performances on challenging surfaces. *Appl Opt* 2018;57:8279–96.